
This manuscript is a preprint and has been submitted for publication in JGR: Earth Surface. Please note that the manuscript has not undergone peer review. Subsequent versions of this manuscript may have different content. If accepted, the final version of this manuscript will be available via the 'Peer-reviewed Publication DOI' link on the right-hand side of this webpage. Please feel free to contact any of the authors. We welcome feedback!

1 **Quantifying Changes in Water Loading in the U.S.**
2 **Southwest via Comparison of GNSS, GRACE, and**
3 **SWE Datasets**

4 **Kenneth C. Gourley¹, Richard A. Bennett^{1,2}, and Christopher Harig¹**

5 ¹Department of Geosciences, The University of Arizona, Tucson, AZ, USA

6 ²Now at NOAA National Geodetic Survey, Silver Spring, MD, USA

7 **Key Points:**

- 8 • GNSS vertical displacements, GRACE TWS, and SWE snowpack estimates are
9 complementary for analyzing surface hydrology
10 • Mountainous GNSS stations are sensitive to snowpack changes, while down basin
11 stations are sensitive to river and lake hydrology
12 • We extract sub-watershed-scale hydrology for the Colorado River Basin by com-
13 bining these three datasets

Corresponding author: Kenneth C. Gourley, kengourley@arizona.edu

14

Abstract

15

16

17

18

19

20

21

22

23

24

25

26

27

28

29

30

31

32

The synthesis of Gravity Recovery and Climate Experiment (GRACE) gravimetry data and Global Navigation Satellite System (GNSS) displacement data provides improved models of surface water hydrology. Much work remains to be done to understand the hydrological signal present in complementary geodetic data in much of the Western U.S., especially the Colorado River basin which comprises a diversity of climates due to its large expanse and highly variable topography. Here, we combine GNSS station vertical displacement data, GRACE surface mass change data, and snow water equivalent (SWE) data to quantify temporal changes in water distribution in the United States (U.S.) Southwest. We focus on a region composed of Arizona, New Mexico, Colorado, and Utah, allowing for the examination of variations in the Colorado River Basin, the primary source of water for the region’s municipalities, agriculture, and ecosystems. We compare these three datasets using surface elastic deformation modeling, and use signal localization techniques to focus on the hydrological signal concentrated within the study region. We demonstrate that the accumulation and melt of snow have a first-order control on the timing of vertical displacement in the region. This is further demonstrated by phase delays between the signals of vertical surface displacement computed from each of the three datasets. These phase delays display a correlation between the distance to the nearest snowpack and the timing of vertical displacement measured at a given GNSS station.

33

Plain Language Summary

34

35

36

37

38

39

40

41

42

43

44

45

46

47

As water and snow accumulate and redistribute on the Earth’s surface, the crust moves elastically in response, similar to placing weights on or removing weights from a rubber band. This elastic motion due to changes in terrestrial water storage (including glaciers, snow cover, lakes, rivers, and groundwater) are small (sub-millimeter to several millimeters per year) but can be measured with modern geophysical techniques. These include the Global Navigation Satellite System (GNSS): a network of sensors installed to measure 3D deformation of the Earth’s surface; and the Gravity Recovery and Climate Experiment (GRACE): two satellite missions that measure changes in the Earth’s gravity field. In this study, we combine measurements from both techniques with existing estimates of the North American snowpack from 2002 to 2023 to quantify watershed basin-scale hydrological features in the southwestern United States. In particular, we observe a difference in timing of when GNSS vs. GRACE is able to sense the distribution of water in various parts of our region. We attribute this to the seasonal storage of water as snow and ice in the mountainous parts of the region.

48

1 Introduction

49

50

51

52

53

54

55

56

57

58

59

60

61

Monitoring and quantifying terrestrial water storage (TWS) throughout the Western United States is essential to water-related policies regarding current and future droughts. Existing measures of drought intensity do not take into account water availability from snow, which is an important driver of hydrological variations in this region (Adusumilli et al., 2019). Geodetic measurements of TWS are produced through the Gravity Recovery and Climate Experiment (GRACE) mission, which determines global gravity variations at monthly intervals (Tapley et al., 2004). Over land, these time-variable gravity fields reflect hydrologic, cryospheric, and atmospheric mass redistribution at monthly and inter-annual time scales and at spatial scales greater than 300 km (Landerer & Swenson, 2012; Swenson & Wahr, 2006). The calculation of the Earth’s response to hydrologic loads using Global Navigation Satellite System (GNSS) stations can help complement the limited spatiotemporal resolution of GRACE TWS measurements (Blewitt et al., 2001; Tregoning & Watson, 2009).

62 Variations in water, snow, and ice on the Earth’s surface result in deformation of the to-
63 pographic and geoidal shapes of the Earth (Han & Razeghi, 2017). Such variations have
64 strong periodic components that produce a mostly elastic response (Farrell, 1972) which
65 appears in both the horizontal and vertical components of GNSS station time series (e.g.
66 van Dam et al., 2007). For regions in which secular changes in TWS occur, the vertical
67 component of GNSS station time series can further be utilized to estimate the magni-
68 tude of these perturbations (e.g. Argus et al., 2017; Knowles et al., 2020). When com-
69 bined with GRACE TWS data, these GNSS vertical displacement data can be used to
70 estimate both the periodic and secular variations in TWS at a finer spatiotemporal scale
71 in a specific region than that available from GRACE alone (Davis et al., 2004; Knappe
72 et al., 2019). Accompanying these benefits, interpretation of GNSS data for hydrogeode-
73 tic applications is complicated by a range of potential sources of periodic motions (e.g.
74 Dong et al., 2002; Chanard et al., 2020; Bogusz et al., 2024), that are presently not well
75 understood and for which there is currently no consensus. In addition to a variety of phys-
76 ical processes, processing methods and analysis models may also contribute to periodic
77 signals observed in GNSS coordinate time series data (e.g. Ray et al., 2007). Bogusz et
78 al. (2024) noted a worldwide annual common mode between IGS Repro3 (Rebischung
79 et al., 2024) and UNR coordinate time series differences, with a median amplitude of the
80 order of 2 mm, peaking in the late summer, which may be explained by different frame
81 realization strategies. These caveats aside, GNSS’s contributions to hydrogeodesy are
82 far reaching (e.g. White et al., 2022, and references therein).

83 While the temporal resolution for an analysis that combines GNSS vertical displacement
84 data and GRACE TWS data can be refined to a daily interval, the spatial resolution is
85 highly dependent on the GNSS station density within a particular region (Adusumilli
86 et al., 2019; Knappe et al., 2019). Studies within regions that have high station densi-
87 ties, such as California, are able to determine TWS changes down to a scale of 10-20 km
88 (Argus et al., 2014, 2017; Carlson et al., 2022). For regions with much sparser station
89 coverage, TWS changes are still resolvable down to a resolution of 50-100 km (Han &
90 Razeghi, 2017). Neither geodetic measurement is optimal for monitoring individual wat-
91 ersheds, but the length scales of their sensitivities prove to be complementary.

92 Joint analysis has been performed for several regions besides California, including Ore-
93 gon and Washington (Fu et al., 2015), the Northern Rockies (Knappe et al., 2019), the
94 Amazon Basin (Davis et al., 2004; Knowles et al., 2020), and Australia (Han & Razeghi,
95 2017). Such studies are able to find good agreement between GNSS vertical displacement
96 data and GRACE TWS data away from mountain ranges. In mountainous regions, in-
97 cluding most of the Western United States, several studies incorporate independent mea-
98 surements of the local snowpack in order to improve their analyses (Argus et al., 2014;
99 Enzminger et al., 2019; Fu et al., 2015; Knappe et al., 2019; Ouellette et al., 2013). When
100 using geodetic data to estimate TWS in such regions, it is necessary to use an accurate
101 snowpack model, as snow water equivalent (SWE) is the dominant signal in those time
102 series (Enzminger et al., 2018). This is especially important when there are other com-
103 peting hydrological signals, such as those from aquifers, that may be out of phase and
104 combine destructively with the SWE signal (Argus et al., 2014, 2017).

105 In this study, we compare GRACE TWS, GNSS vertical displacement, and SWE datasets
106 in the Southwest United States (Figure 1) to determine the extent to which the spatiotem-
107 poral resolution of GRACE TWS models can be enhanced. Although previous work has
108 created a refined TWS model using GRACE and GNSS datasets for the conterminous
109 United States (Adusumilli et al., 2019), hydrological signals present in geodetic data from
110 the Southwest United States are dominated by changes in snowpack SWE. Additionally,
111 the spacing of continuously-operating GNSS stations is irregular in this region, making
112 regional variations difficult to observe. We overcome this challenge by using a data lo-
113 calization technique based on Slepian basis functions (Harig & Simons, 2012; Simons &
114 Dahlen, 2006). We demonstrate regional- and watershed-scale changes in TWS and quan-

115 tify the contribution of the snowpack SWE signal to the overall GRACE TWS model
116 for the study region.

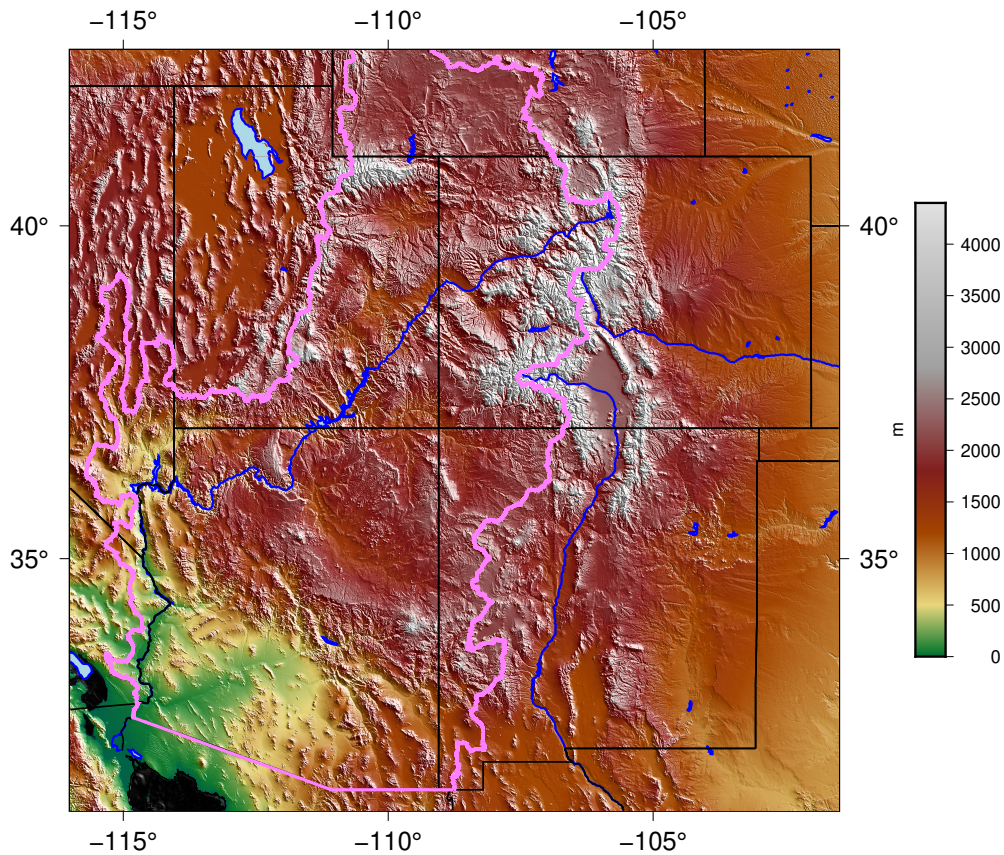


Figure 1. Plot of the surface topography of the Southwest United States. The black lines are state and federal borders; the blue lines are major rivers; and the pink line is the boundary of the Colorado River Basin. The study region – composed of the states of Arizona, New Mexico, Colorado, and Utah – contains varying elevations and multiple mountainous areas. The major rivers in the study region are the Colorado (center), Arkansas (center right), and Rio Grande (bottom right). The mountain ranges which accommodate the majority of the fall and winter snowpack are the Rocky Mountains, which extend through central and western Colorado and northern New Mexico; and the Wasatch and Uinta Ranges, which extend from central to northern Utah. These same ranges also supply snowmelt to the upper Colorado River Basin, which then flows down to the Gulf of California (Zeng et al., 2018).

117 2 Methods

118 2.1 GNSS Displacements

119 We use GNSS displacements from 266 heterogeneously-spaced, continuously-operating
120 stations across Arizona, New Mexico, Colorado, and Utah (Figure 2). Most of these sta-
121 tions were installed between 2005 and 2010. The final orbit daily GNSS solutions for ver-
122 tical displacement were processed by the University of Nevada Reno’s Nevada Geode-

123 tic Laboratory (UNR; <http://geodesy.unr.edu/>). These solutions were generated using
124 GIPSY-OASIS II utilizing the Jet Propulsion Laboratory’s orbital products, the FES2004
125 ocean tide model, and solid Earth tides from IERS 2010 conventions. We use daily posi-
126 tions products given in the International Terrestrial Reference Frame 2014 (Altamimi
127 et al., 2016). Further information on the processing method utilized by UNR can be found
128 in Blewitt et al. (2018). The precision of the vertical signal varies daily for each station,
129 with formal error usually 1–2 mm, and these daily uncertainties are propagated into the
130 time series.

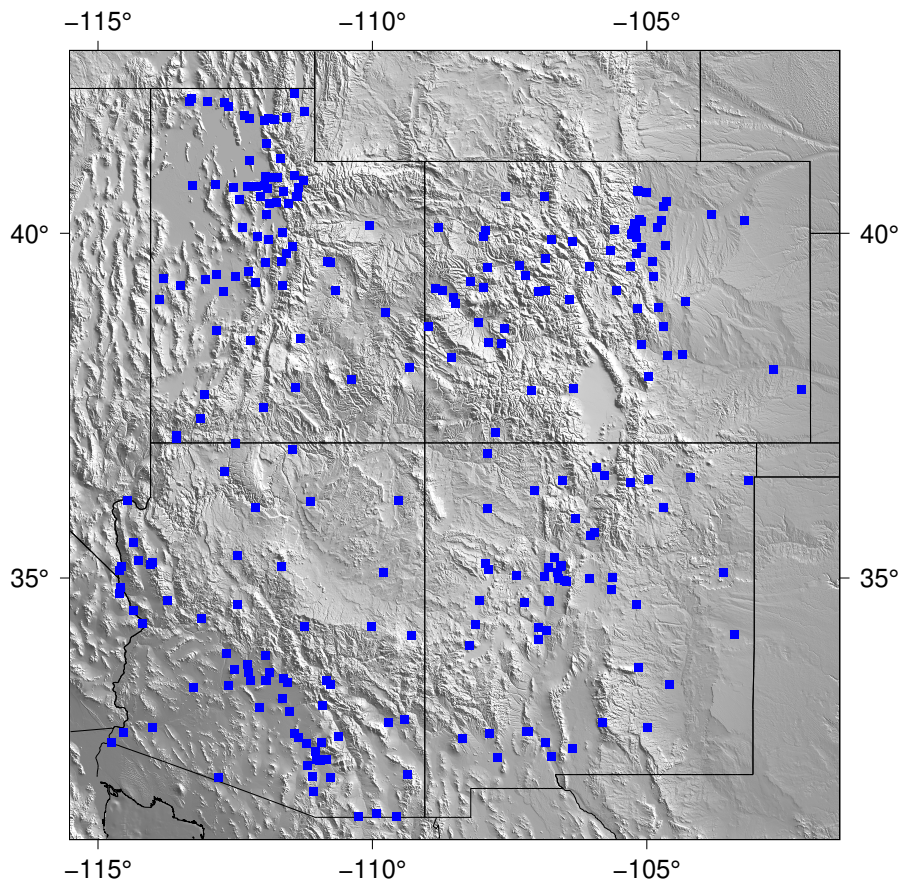


Figure 2. Map of the study region topography with the GNSS station locations used in this study plotted as blue squares. Station density is high in most mountainous parts of this region, as well as in the Basin and Range. However, station coverage is not uniform and is quite poor on the Colorado Plateau and in the eastern parts of Colorado, Utah, and New Mexico.

131 After downloading the GNSS station data, we use Hector (<http://segal.ubi.pt/hector/>)
132 to remove outliers and jumps from each station’s vertical displacement time series (Bos
133 et al., 2013). Outliers are single data points that fall outside of the statistical trend of
134 each station’s time series. Jumps are sudden shifts in the statistical trend that can come
135 from a variety of sources, primarily earthquakes and changes in station antennas. Out-
136 liers and jumps frequently plague GNSS station time series, and their removal greatly
137 improves the intercomparisons with the GRACE and UASWE displacement time series
138 used in this study.

2.2 GRACE Time-variable Gravimetry

We use monthly GRACE RL-06 and GRACE Follow-On RL-06.2 data (collectively referred to as GRACE data in this paper) through September 2023 from the Center for Space Research at the University of Texas at Austin. These data are distributed as Stokes coefficients to degree and order 60. Degree 2 and 3 order 0 coefficients are replaced with those from GRACE Technical-Note 14, which are derived from satellite laser ranging (Loomis et al., 2020). Degree 1 coefficients are added from GRACE Technical-Note 13, representing estimated geocenter variations (Sun et al., 2016; Swenson et al., 2008). We transform the geopotential into surface mass density using the method of Wahr et al. (1998) to account for the surface deformation resulting from surface mass changes.

We localize the GRACE data to the study region using Slepian functions (Harig & Simons, 2012; Simons & Dahlen, 2006). The study region here is defined by the area enclosed by the combined governmental borders of the four Colorado Plateau states: Arizona, New Mexico, Colorado, and Utah (Figure 1). We also include a 0.5 degree buffer around the region to mitigate any effects from GNSS stations very near the region boundary. This Slepian method allows for the spatio-spectral concentration of data within in an arbitrary region on a sphere and has been successfully applied to GRACE data to study mass changes in ice sheets and mountain glaciers (e.g. Harig & Simons, 2015, 2016; Beveridge et al., 2018; von Hippel & Harig, 2019). Each Slepian function is a solution to an eigenvalue equation that optimizes the localization within a region. The associated eigenvalue is a measure of concentration within this region. We create a basis using only the well-concentrated functions. This sparse representation of data allows for the creation of models that experience very little influence from phenomena outside of the region of interest. The localized surface density fields are then expanded on a 0.25° grid for use with LoadDef.

2.3 Snow Water Equivalent Product

The University of Arizona snow water equivalent product (UASWE) (Zeng et al., 2018) dataset is composed of daily measurements of SWE across the conterminous US. These measurements are given on a regularly-spaced grid with a resolution of 4 km. The data spans from October 1981 to September 2023, although this study focuses on the subset of measurements that overlaps in time with GRACE data. The UASWE dataset is constructed by assimilating in-situ measurements of SWE and snow depth with gridded precipitation and temperature data across the conterminous US (Zeng et al., 2018).

Similar to our processing of GRACE data, we project the UASWE spatial fields into the same $L = 60$ Slepian basis localized to the four state study region. This spatially band-limits the UASWE dataset for consistent comparison between the two datasets. The regionalized dataset is then re-gridded at a regular interval of 0.25° for use in LoadDef.

2.4 Conversion to Displacement Measurements and Time Series Modifications

We use the software package LoadDef (<https://github.com/hrmartens/LoadDef>) to compute vertical surface displacements resulting from the regionalized GRACE and UASWE surface mass distribution datasets. LoadDef produces analytical models of surface mass loading for a spherically symmetric, non-rotating, elastic, and isotropic planet (Martens et al., 2019). Load Love numbers (Love, 1909) are computed based on a model of densities and seismic-wave velocities for Earth as a function of radius; PREM (Dziewonski & Anderson, 1981) is chosen as the model for both parameters in this study. Load Green's functions (Farrell, 1972) are then computed based on the load Love numbers. Lastly, to derive the surface displacement response, the load Green's functions are integrated and multiplied by the gridded load height and density for an input surface mass distribution.

188 This LoadDef Earth model is the same one that we use to compute the surface density
189 of the GRACE time-variable gravity dataset. The density of water, 1000 kg/m^3 , is cho-
190 sen for both GRACE and UASWE, as both datasets are given as a water equivalent. The
191 displacement response for both surface mass distribution datasets is computed at each
192 GNSS station location for easy comparison between all three datasets. Before the UASWE
193 dataset is passed as input to LoadDef, the monthly average load is computed using the
194 same monthly endpoints as used by the GRACE dataset. This reduces the computational
195 load of running the LoadDef routines for two datasets over 276 months at 266 station
196 locations.

197 All three time series are temporally smoothed using radial basis functions (RBFs) as smooth-
198 ing functions followed by interpolation at a daily interval. The RBF routine used is from
199 the scikit-learn software package (<https://scikit-learn.org/>), which optimizes kernels over
200 a range of input time scales (Pedregosa et al., 2011). A range of 0.5 to 10 years is selected
201 to form the RBF kernels for this study, as this range captures the intra- and inter-annual
202 variations present in all three datasets. These datasets are primarily dominated by a pe-
203 riodicity of one year. For consistency between datasets, the same set of RBF kernels is
204 applied to all three vertical displacement time series. This low-pass filtering scheme serves
205 to overcome the challenge presented by small gaps in the daily GNSS station data and
206 monthly gaps in the GRACE data. The kernels also provide a low-pass filter for the datasets,
207 resulting in the suppression of daily and weekly variations in the time series. These vari-
208 ations are likely not the result of elastic surface loading due to changes in hydrology, which
209 is the focus of this study (Adusumilli et al., 2019; Farrell, 1972). After applying the RBF
210 kernels to the three displacement datasets, the time series are then re-sampled at a daily
211 interval.

212 2.5 Data Intercomparisons

213 Three new data products are created in this study in order to examine the effects of vari-
214 ations in hydrology on geodetic datasets in the Southwest United States: a) phase de-
215 lays between vertical GNSS time series and computed GRACE vertical displacement data;
216 b) least-squares regressions between vertical GNSS time series and computed UASWE
217 vertical displacement; and c) least-squares regressions between computed GRACE and
218 UASWE vertical displacement data. Each of these products is evaluated at the 266 GNSS
219 station locations in the study area.

220 Before creating these products, each of the three displacement datasets is aligned in time
221 at each station location. The time series are then sliced such that only the overlap be-
222 tween the pertinent time series is analyzed. We choose a minimum overlap of three years
223 between the GNSS and GRACE time series. This results in short intervals of overlap at
224 some stations when comparing the GNSS and GRACE vertical displacement datasets,
225 as some GNSS stations were deployed relatively recently. These short intervals are a cause
226 of the poor cross-correlation observed when computing the phase delays between these
227 two time series at some station locations. Each time series is also de-trended by remov-
228 ing the mean and standard deviation before proceeding with computing the phase de-
229 lays or least-squares regressions.

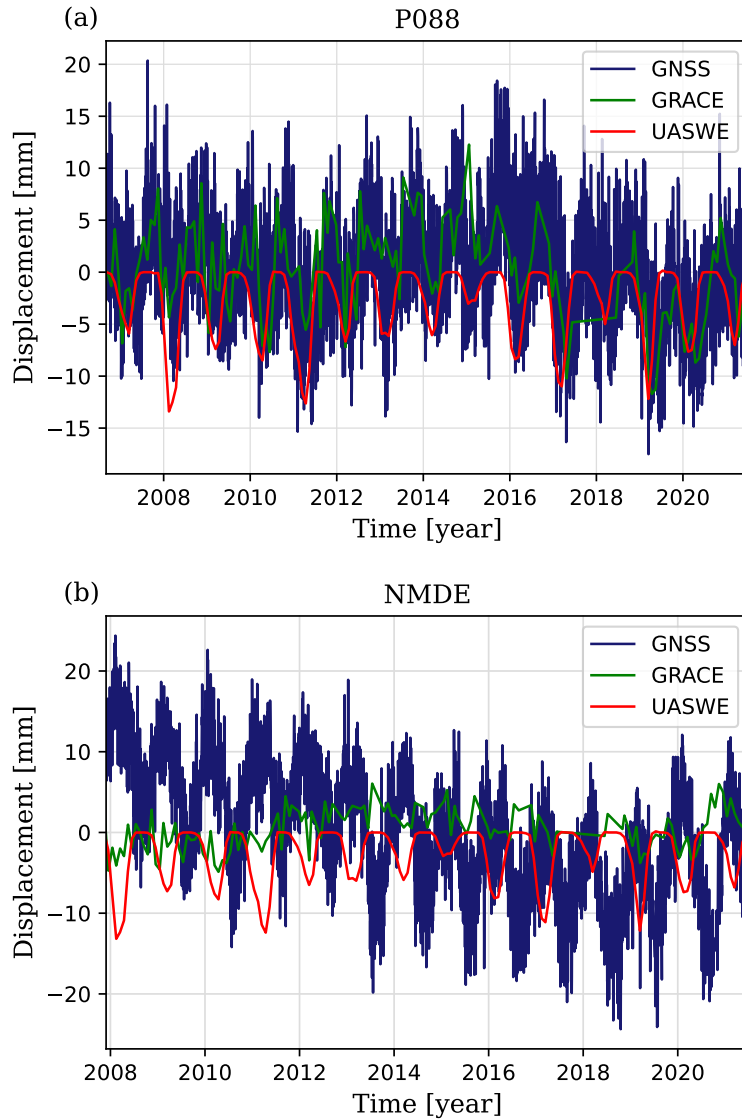


Figure 3. Plot of the vertical displacement time series at GNSS stations (a) P088 and (b) NMDE for the three datasets used in this study. The original GNSS daily vertical displacement is plotted in blue, while the computed vertical displacements due to elastic loading from the GRACE TWS and UASWE snowpack SWE datasets are plotted in green and red, respectively. (a) P088 is located in the upper elevations of the Wasatch Range. The periodic annual amplitude of vertical deformation for the GNSS time series is around ± 15 mm, while the equivalent computed amplitudes for the GRACE and UASWE time series are lower, at ± 8 mm and -10 to 0 mm, respectively. These annual periods are close to being in-phase at this station, with GRACE lagging UASWE by about 20 days and GNSS lagging GRACE by 14 days. The high correlation between the GRACE and GNSS displacement suggests that the variations in the vertical signal at this GNSS station are explained almost entirely by variations in surface water mass. (b) NMDE is located in a valley in southwest New Mexico. The periodic annual amplitude of vertical deformation for the GNSS time series is around ± 20 mm, while the equivalent computed amplitudes for the GRACE and UASWE time series are lower, at ± 5 mm and -10 to 0 mm, respectively. The annual responses computed from GRACE TWS and the UASWE snowpack are significantly lower at this location, owing to station's distance from the nearest high mountain range. The annual periodic signals in the GNSS and GRACE datasets are almost completely antiphase, with GRACE leading GNSS by 214 days. While the low-spatial-resolution GRACE dataset is sensitive to changes in the broader regional snowpack, station NMDE is sensitive to the snowmelt runoff that flows within its vicinity during the spring and summer months.

230 The GRACE-GNSS phase delays highlight the additional hydrological resolution that
231 vertical GNSS station displacements can provide when combined with GRACE surface
232 water loading data. When comparing Figures 3(a) and 3(b), it becomes apparent that
233 the phase difference between the GNSS and GRACE time series is not uniform among
234 station locations. These phase delays are computed by cross-correlating the de-trended
235 GNSS and GRACE vertical displacement datasets. Any computed phase delays longer
236 than six months are removed. Because the primary periodic signal in both datasets is
237 approximately annual, any computed phase delay longer than half this period is due to
238 poor correlation and not representative of any physical process. The final set of phase
239 delays is then projected into the same local Slepian basis used for the GRACE and UASWE
240 datasets in the study region and plotted.

241 We compute two regression products by performing a least-squares regression using the
242 UASWE vertical displacement data values as the independent variable for both. These
243 regressions are performed at each station location. One regression uses the GNSS ver-
244 tical displacement data values as the dependent variable, and the other uses the GRACE
245 vertical displacement data values. The resulting R^2 value of fit for the regression at each
246 station location is then the measure of the percentage of variation in the dependent vari-
247 able that can be explained by variation in the independent variable. This statistical anal-
248 ysis presents a method of determining how strongly GNSS vertical displacement and GRACE
249 TWS are determined by changes in snowpack SWE within the study region. High val-
250 ues of R^2 indicate that snowpack SWE is the dominant driver of surface elastic defor-
251 mation, while low values indicate that a different physical process must control the dis-
252 placement at a given location. These two regression products at the stations are then
253 projected into the same Slepian basis as described above and plotted separately.

254 3 Results and Analysis

255 3.1 Phase Delays

256 The result of the phase delay computation between the GNSS and GRACE vertical dis-
257 placement datasets is shown in Figure 4. Of the 266 GNSS stations used in this study,
258 259 produce phase delays through cross-correlation with the GRACE vertical displace-
259 ment dataset. Of these 259 phase delays, only 110 are less than six months; these are
260 the phase delays plotted in Figure 4. The phase delays are mostly coherent in the var-
261 ious sub-regions of the study area. In Colorado, phase delays are scattered around -60
262 days, indicating that GNSS stations in this sub-region sense vertical motion around two
263 months in advance of GRACE satellite gravimetry. In Utah, phase delays are scattered
264 around 0 days, with most being slightly negative, suggesting that, in this sub-region, GNSS
265 stations and GRACE satellite gravimetry sense changes in elastic deformation due to sur-
266 face water loading at around the same time. In Arizona, phase delays are mostly scat-
267 tered around 90 days, indicating that GNSS stations in this sub-region sense changes in
268 elastic deformation due to surface water loading months after it is perceived by GRACE
269 satellite gravimetry. Phase delays are widely scattered in New Mexico, with many around
270 -120 days and other around 80 days. This suggests that there is little consistency among
271 GNSS station responses in this sub-region.

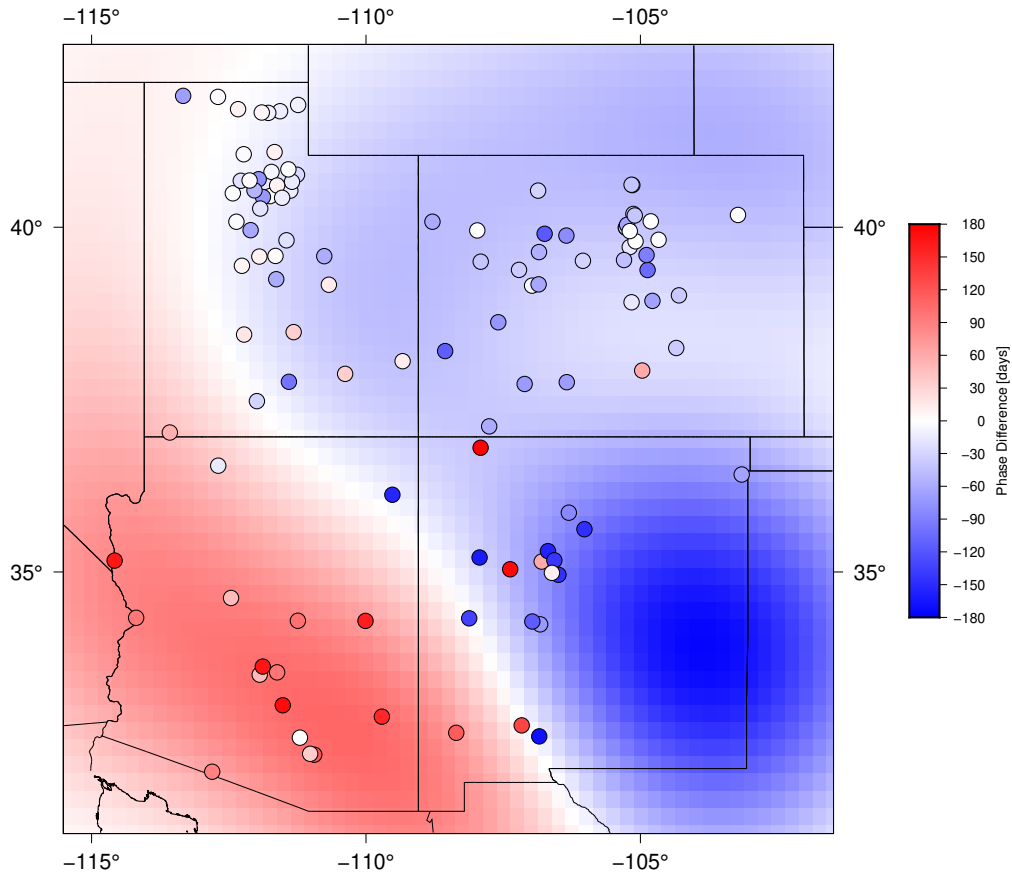


Figure 4. Map of phase differences between the observed GNSS and computed GRACE vertical displacement datasets. The phase delay at individual station locations is plotted as filled circles. The long-wavelength response computed by projecting the location responses into the regional Slepian basis is plotted across the entire map. A negative phase difference (blue) indicates that the annual periodic signal of GNSS is leading that of GRACE, while a positive phase difference (red) indicates that the GRACE signal is leading that of GNSS. There exists a strong degree two signal in the regional phase differences: GNSS stations sense hydrological loading in the mountainous regions one to two months before it appears in the GRACE gravimetry data, while this relative timing flip-flops in the lower Colorado River Basin.

272 Overall, the Slepian projection of the phase delays into the study region agrees with the
 273 individual phase delay results. This paints the broad picture that GNSS stations in and
 274 around mountainous areas of the Southwest United States respond to elastic deforma-
 275 tion due to surface water loading months in advance of GNSS stations in low-lying and
 276 desert areas. GNSS stations in Colorado in Utah sense the accumulation of snow in fall
 277 and winter months, while stations in Arizona sense the runoff from the melting snow-
 278 pack in lower parts of mountain watersheds during spring months. The negative phase
 279 delay anomaly in New Mexico likely does not represent a real physical feature, as it is
 280 heavily skewed by several negative-valued station locations contained within it. Ignor-
 281 ing this feature, a two-lobed pattern of phase delays emerges, with a negative lobe in the
 282 north and northeast parts of the study region, and a positive lobe in the southwest por-
 283 tion. It is important to note that, due to the low spatial resolution of GRACE TWS data,

284 it provides only a snapshot into broad regional hydrological processes. By combining in-
285 formation about elastic deformation from both GRACE and GNSS, details about watershed-
286 scale hydrological processes materialize.

287 **3.2 GNSS and UASWE Regression**

288 The result of the least-squares regression between the observed GNSS and computed UASWE
289 vertical displacement time series is shown in Figure 5. The variance in GNSS vertical
290 displacement data explained by vertical displacement computed from the UASWE dataset
291 for most stations is below 10%. For some sub-regions, especially in the Wasatch Range
292 and the Rocky Mountains, 20-30% of the variance observed at many stations is explained
293 by the UASWE dataset. These station locations primarily correlate with the mountain-
294 ous regions of the study area. A handful of stations have around 50% of their variance
295 explained by the UASWE dataset. These stations are highly sensitive to the accumu-
296 lation and melt of the local snowpack.

297 The overall low variance explanation from the UASWE dataset is due to the fact that
298 this dataset records only the accumulation and removal of snow in the snowpack itself.
299 It does not provide information about the redistribution of snowpack meltwater that forms
300 in the spring months. Figure 5 demonstrates that a large portion of the GNSS stations
301 in the study area are more sensitive to the surface elastic deformation that results from
302 the local accumulation of meltwater as opposed to changes in the snowpack itself. The
303 GNSS stations essentially act as spatial high-pass filters for the elastic deformation, as
304 they are responsive to TWS variations only within tens of kilometers, as suggested by
305 these results. They can provide much higher resolution TWS data for a hydrologically
306 complex region such as the Southwest United States, even though the station density is
307 sparse and irregular.

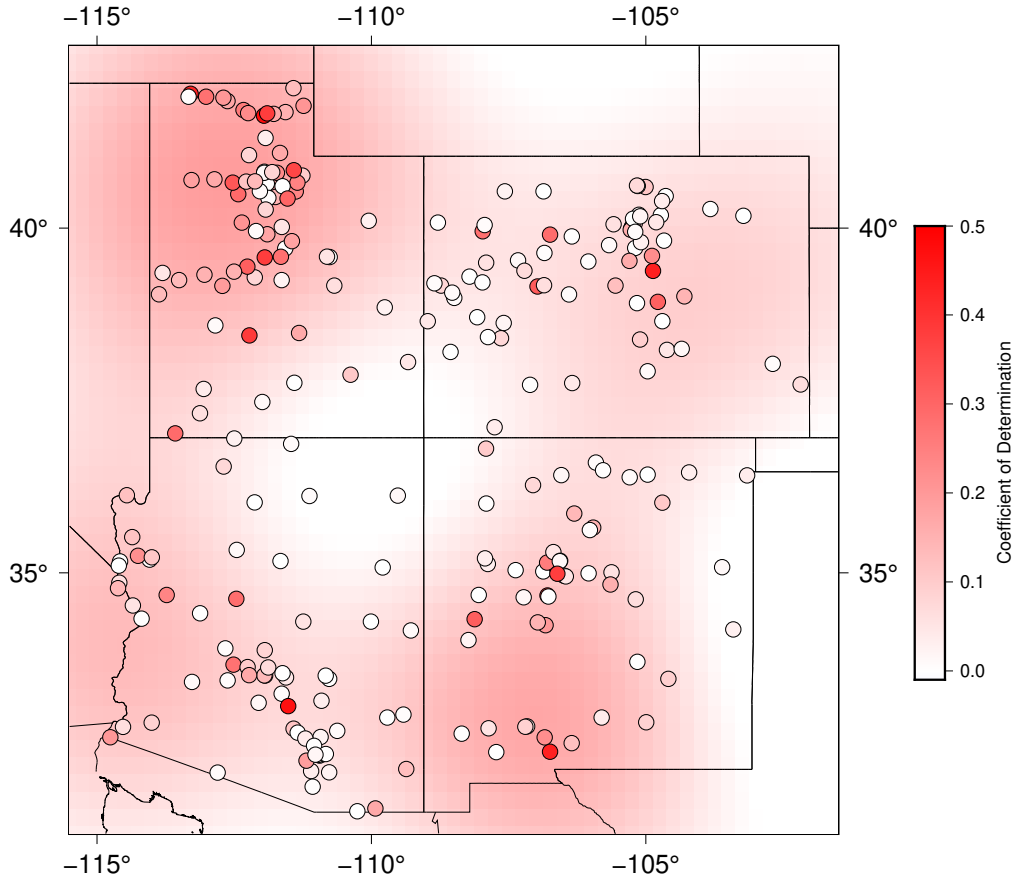


Figure 5. Map of the R^2 value (coefficient of determination) that results from performing a least-squares regression between the observed GNSS and computed UASWE vertical displacement time series values at each station location. The R^2 value at each individual station location is plotted as a filled circle, and the response computed by projecting the site responses into the regional Slepian basis is plotted across the entire map. There is little coherence between the two datasets across the study area, as only about 30 locations have an R^2 value above 0.2. The relative GNSS station spacing is reflected in the regional projection, as the background map has the highest values in the sub-regions with the densest populations of stations, while the center of the region has the fewest stations and therefore the lowest R^2 values.

308

3.3 GRACE and UASWE Regression

309

310

311

312

313

314

315

316

317

318

As seen in Figure 6, the least-squares regression between the computed GRACE and UASWE vertical displacement time series is significantly more uniform than the regression shown in Figure 5. This is to be expected, as the GRACE TWS dataset has low spatial resolution, and most of the pixels in the study area behave coherently. Most station locations have GRACE vertical displacement time series variance that are explained by variance in the UASWE vertical displacement time series in excess of 40%. Many of these stations have values around 50%, which is excellent considering that the UASWE dataset does not contain information about the elastic deformation due to the redistribution of snowpack meltwater. It is this meltwater that drives the majority of surface elastic deformation in the spring and summer months. The only sub-regions where the GRACE

319 TWS data shows significant divergence from the UASWE data are the areas in south-
 320 321 322 323 324 325 326
 320 southern and northwestern Arizona. These locations are sufficiently far away enough from the
 321 mountainous parts of the study region and their associated watersheds that the stations'
 322 signals are not coupled to the region's snowpack. Given that the variance in GRACE
 323 vertical displacement data explained by the variance in UASWE vertical displacement
 324 data in these sub-regions Arizona is around 10%, these stations might be decoupled to
 325 the broader hydrological processes of the study region and may reflect some sensitivity
 326 to elastic deformation resulting from precipitation from the North American Monsoon.

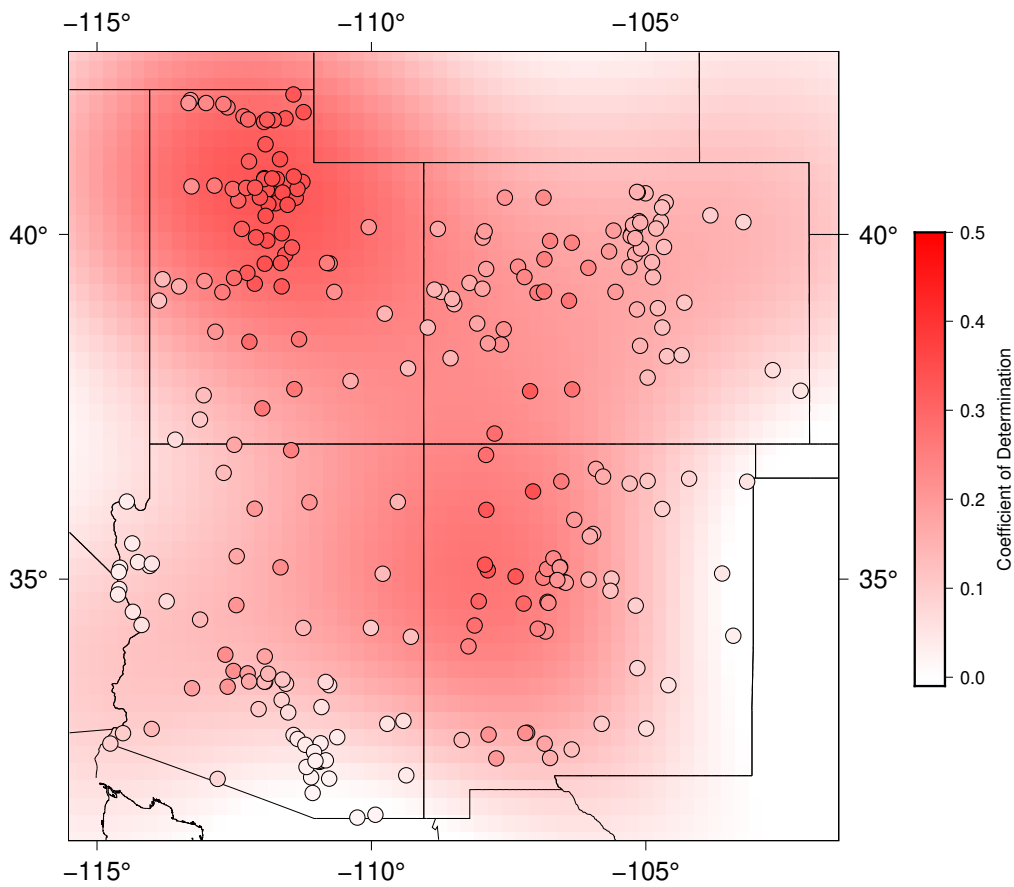


Figure 6. Same as Figure 5 but for the R^2 values that result from the linear regression between the computed GRACE and UASWE vertical displacement time series values at each station. In contrast to Fig. 5, there is strong coherence between the two datasets across the study area at most sites. This suggests that the snowpack provides a first-order control on GRACE TWS data. The only exceptions are two groups of stations in southern Arizona and along the Colorado River in western Arizona. These groups of stations have R^2 values near 10%, suggesting that they are not highly controlled by variations in the snowpack.

4 Discussion

4.1 Complementary Data

This study demonstrates the utility of combining GNSS vertical displacement, SWE, and GRACE TWS data for refining the spatiotemporal resolution of hydrological phenomena in a localized region. The spatial and temporal resolutions of GNSS displacement and GRACE gravimetry data are complementary. GNSS stations are sensitive to hyper-local elastic deformation occurring on scales of kilometers to tens of kilometers, while GRACE gravimetry data provides information about regional and continental TWS trends (Landerer & Swenson, 2012; Swenson & Wahr, 2006). GNSS station time series are available at a daily interval and can provide near-real-time information about local variations in TWS (Fu et al., 2015). Meanwhile, GRACE provides information on long-term trends in TWS, such as inter-annual variability in drought conditions (e.g. Enzinger et al., 2019).

Such near-real-time monitoring of TWS is becoming increasingly important as the effects of anthropogenic climate change increase in severity (Jiang et al., 2021). This is especially apparent in the study area, where water storage along the Colorado River is reaching extreme lows (Adusumilli et al., 2019). Instead of relying on streamflow measurements during the spring months, models of elastic deformation that incorporate GNSS vertical displacement and Gravity Recovery and Climate Experiment Follow-On (GRACE-FO) TWS data can help refine estimates of the snowpack in the source regions of the Colorado River during the fall and winter months. This would help governments that rely on the Colorado River for water to plan water savings and other emergency measures months in advance of a water shortage.

A high density of GNSS stations is critical to monitoring changes in TWS throughout a region (Han & Razeghi, 2017; Knappe et al., 2019). However, the results of this study suggest that it is possible to partially complement areas of sparse GNSS networks with snowpack SWE models in mountainous regions, such as the Western United States. These snowpack SWE models provide information about snow accumulation and melt, which is critical to understanding surface elastic deformation in the mountain ranges that receive snow. This same information is not fully conveyed by GNSS station vertical displacement data, as suggested by Figure 5. On the other hand, GNSS stations in drainage areas around these mountain ranges provide data on the timing and magnitude of snowmelt runoff. The placement of GNSS stations in different segments of larger watersheds is integral to understanding TWS variations at the watershed basin scale. It is the intent of this and future studies to motivate the deployment and maintenance of denser GNSS networks to monitor TWS throughout the Western United States and other regions.

4.2 Sources of Error

When analyzing GNSS station displacement data, it is important to take into account various sources of error. These include atmospheric delay modelling (Tregoning et al., 2009), site-specific thermal expansion (Fang et al., 2013; Yan et al., 2009), poroelastic strain due to groundwater (Tsai, 2011), and other non-tidal errors (Gu et al., 2017). Previous studies also removed stations from their analyses whose locations have large local soil expansion and contraction responses due to changes in groundwater storage (e.g. Argus et al., 2014, 2017). No such selectivity is performed in this study, and it is likely that the stations that display large discrepancies in their signal content compared to GRACE are biased by one or more of the site-specific errors listed above. Future analyses using this GNSS vertical displacement dataset will first remove stations with high variability in their response to surface water loading using a methodology similar to Argus et al. (2017). GNSS station displacement errors other than the ones mentioned will also be considered, such as those summarized in Dong et al. (2002).

4.3 Regional Implications

Besides variations in TWS, the data in this study provides useful information about other climate trends and phenomena. As mentioned previously, one of the most pertinent contributions to TWS in the study area besides snow accumulation and melt is the North American Monsoon. One interesting result to emerge from the analyses in this study is the identification of a subset of GNSS stations whose vertical displacement is decoupled from changes in the snowpack relative to the majority of the stations in this study. These stations in southern and northwestern Arizona, as highlighted in Figure 6, should be investigated for their relationship to monsoonal precipitation. Future analyses will involve attempting to separate the seasonal signal of the North American Monsoon from the annual signal of snow accumulation and melt in the Southwest United States. A focus on other climate patterns, such as the El Niño-Southern Oscillation and atmospheric rivers, may also prove fruitful (Adusumilli et al., 2019).

The ultimate goal of this line of work is to create a model of sub-monthly variations in TWS with a spatial resolution of tens of kilometers in the study region. This will involve a joint inversion of GNSS and GRACE datasets, similar to Han & Razeghi (2017) and Knappe et al. (2019). A snowpack SWE dataset will also be necessary for the analysis, as demonstrated by this study, to provide the desired spatial resolution. That being said, the snowpack SWE dataset does not make up for the station sparsity in low elevation areas of the study region. In order to model the redistribution of snowmelt runoff throughout the study region, another TWS dataset is required. One such candidate dataset is the Global Land Data Assimilation System (GLDAS), which provides 1 km resolution land-based grids of changes in surface water resources (Rodell et al., 2004). This dataset could be incorporated in a joint analysis, although previous studies (e.g. Fu et al., 2015; Knappe et al., 2019) suggest that GLDAS has a limited representation of the water cycle and provides little information that is independent of SWE datasets.

5 Conclusions

In this study, we perform the first region-specific analysis and comparison of GNSS vertical displacement, GRACE TWS, and snowpack SWE datasets for the southwest United States. We observe a location-dependent phase delay between GNSS and GRACE vertical displacement data, demonstrating that snow accumulation and melt in mountainous regions provide a first-order control on elastic deformation of Earth’s surface in this study area. Hydrological surface loading from the North American Monsoon is also suggested as a second-order control on the observed displacement at GNSS stations in southern and northwestern Arizona. Variations in the UASWE snowpack SWE coverage dataset are observed to have little control over variations in GNSS vertical displacement data, indicating that GNSS stations in the study region have a hyper-local sensitivity to variations in the distribution of TWS surface mass. A model of the redistribution of snowmelt runoff in individual watersheds is needed to complement TWS deficiencies in the UASWE dataset. Future work is needed to create a joint inversion of these datasets to pursue near-real-time monitoring of TWS variations as well as insights into other climate trends that may be present in the data.

Open Research Section

The code used in this work is available freely online (Harig et al., 2015) as part of the SLEPIAN code package. Specifically Slepian_alpha (Simons et al., 2020) and Slepian_bravo (Simons & Harig, 2020) are used to generate and work with Slepian functions, while Slepian_delta (Harig & Simons, 2022) processes GRACE data. Installation instructions for the various Slepian code repositories can be found at <http://github.com/Slepian/Slepian> (Plattner et al., 2023). The GNSS time series (Blewitt et al., 2018) used for processing in this study are available from the University of Nevada Reno Nevada Geodetic Lab-

427 oratory (<http://geodesy.unr.edu/>) under open access. Version 1.9 of Hector (Bos et
428 al., 2013) used to compute linear displacement trends for the GNSS time series is avail-
429 able via the GNU General License at <https://segal.ubi.pt/webservices/whatishector/>.
430 The CSR RL06 GRACE time series used for processing in this study are freely available
431 at The NASA Physical Oceanography Distributed Active Archive Center (PO.DAAC)
432 (<https://podaac.jpl.nasa.gov/>).

433 Acknowledgments

434 CH acknowledges support from the National Science Foundation (NSF) via grant NSF-
435 2142980 funded by the Geophysics program. Figures were plotted using the Generic Map-
436 ping Tools (Wessel et al., 2013).

437 References

- 438 Adusumilli, S., Borsa, A. A., Fish, M. A., McMillan, H. K., & Silverii, F. (2019). A
439 Decade of Water Storage Changes Across the Contiguous United States From
440 GPS and Satellite Gravity. *Geophys. Res. Lett.*, *46*(22), 13006–13015. doi:
441 10.1029/2019GL085370
- 442 Altamimi, Z., Rebischung, P., Métivier, L., & Collilieux, X. (2016). ITRF2014:
443 A new release of the International Terrestrial Reference Frame modeling non-
444 linear station motions. *J. Geophys. Res. Solid Earth*, *121*(8), 6109–6131. doi:
445 10.1002/2016JB013098
- 446 Argus, D. F., Fu, Y., & Landerer, F. W. (2014). Seasonal variation in total water
447 storage in California inferred from GPS observations of vertical land motion. *Geo-*
448 *phys. Res. Lett.*, *41*, 1971–1980. doi: 10.1002/2014GL059570
- 449 Argus, D. F., Landerer, F. W., Wiese, D. N., Martens, H. R., Fu, Y., Famiglietti,
450 J. S., . . . Watkins, M. M. (2017). Sustained Water Loss in California’s Moun-
451 tain Ranges During Severe Drought From 2012 to 2015 Inferred From GPS. *J.*
452 *Geophys. Res. Solid Earth*, *122*(12), 10559–10585. doi: 10.1002/2017JB014424
- 453 Beveridge, A. K., Harig, C., & Simons, F. J. (2018). The changing mass of glaciers
454 on the Tibetan Plateau, 2002–2016, using time-variable gravity from the GRACE
455 satellite mission. *J. Geodetic Sci.*, 1–15. doi: 10.1515/jogs-2018-0010
- 456 Blewitt, G., Hammond, W., & Kreemer, C. (2018). Harnessing the GPS Data Explo-
457 sion for Interdisciplinary Science. *Eos*, *99*. doi: 10.1029/2018eo104623
- 458 Blewitt, G., Lavallée, D., Clarke, P., & Nurutdinov, K. (2001). A new global mode
459 of earth deformation: Seasonal cycle detected. *Science*, *294*(5550), 2342–2345. doi:
460 10.1126/science.1065328
- 461 Bogusz, J., Rebischung, P., & Klos, A. (2024). Differences in annual signals
462 between igs- and ngl-derived position time series: testing different strategies
463 of alignment to the reference frame. In *EGU General Assembly 2024*. doi:
464 10.5194/egusphere-egu24-5351
- 465 Bos, M. S., Fernandes, R. M., Williams, S. D., & Bastos, L. (2013). Fast error anal-
466 ysis of continuous GNSS observations with missing data. *J. Geod.*, *87*(4), 351–360.
467 doi: 10.1007/s00190-012-0605-0
- 468 Carlson, G., Werth, S., & Shirzaei, M. (2022). Joint Inversion of GNSS and GRACE
469 for Terrestrial Water Storage Change in California. *J. Geophys. Res. Solid Earth*,
470 *127*(3). doi: 10.1029/2021jb023135
- 471 Chanard, K., Métois, M., Rebischung, P., & Avouac, J.-P. (2020). A warning against
472 over-interpretation of seasonal signals measured by the Global Navigation Satellite
473 System. *Nature Communications*, *11*, 1375. doi: 10.1038/s41467-020-15100-7
- 474 Davis, J. L., Elósegui, P., Mitrovica, J. X., & Tamisiea, M. E. (2004). Climate-
475 driven deformation of the solid Earth from GRACE and GPS. *Geophys. Res.*
476 *Lett.*, *31*(24), 1–4. doi: 10.1029/2004GL021435

- 477 Dong, D., Fang, P., Bock, Y., Cheng, M. K., & Miyazaki, S. (2002). Anatomy of ap-
478 parent seasonal variations from GPS-derived site position time series. *J. Geophys.*
479 *Res. Solid Earth*, *107*(B4), 1–16. doi: 10.1029/2001jb000573
- 480 Dziewonski, A. M., & Anderson, D. L. (1981). Preliminary reference Earth model.
481 *Phys. Earth Planet. Inter.*, *25*(4), 297–356. doi: 10.1016/0031-9201(81)90046-7
- 482 Enzinger, T. L., Small, E. E., & Borsa, A. A. (2018). Accuracy of Snow Water
483 Equivalent Estimated From GPS Vertical Displacements: A Synthetic Loading
484 Case Study for Western U.S. Mountains. *Water Resour. Res.*, *54*(1), 581–599. doi:
485 10.1002/2017WR021521
- 486 Enzinger, T. L., Small, E. E., & Borsa, A. A. (2019). Subsurface Water Dominates
487 Sierra Nevada Seasonal Hydrologic Storage. *Geophys. Res. Lett.*, *46*(21), 11993–
488 12001. doi: 10.1029/2019GL084589
- 489 Fang, M., Dong, D., & Hager, B. H. (2013). Displacements due to surface tempera-
490 ture variation on a uniform elastic sphere with its centre of mass stationary. *Geo-*
491 *phys. J. Int.*, *196*(1), 194–203. doi: 10.1093/gji/ggt335
- 492 Farrell, W. E. (1972). Deformation of the Earth by surface loads. *Rev. Geophys.*,
493 *10*(3), 761–797. doi: 10.1029/RG010i003p00761
- 494 Fu, Y., Argus, D. F., & Landerer, F. W. (2015). GPS as an independent
495 measurement to estimate terrestrial water storage variations in Washington
496 and Oregon. *J. Geophys. Res. Solid Earth*, *120*, 552–566. doi: 10.1002/
497 2014JB011415.Received
- 498 Gu, Y., Fan, D., & You, W. (2017). Comparison of observed and modeled seasonal
499 crustal vertical displacements derived from multi-institution GPS and GRACE
500 solutions. *Geophys. Res. Lett.*, *44*(14), 7219–7227. doi: 10.1002/2017GL074264
- 501 Han, S. C., & Razeghi, S. M. (2017). GPS Recovery of Daily Hydrologic and
502 Atmospheric Mass Variation: A Methodology and Results From the Aus-
503 tralian Continent. *J. Geophys. Res. Solid Earth*, *122*(11), 9328–9343. doi:
504 10.1002/2017JB014603
- 505 Harig, C., Lewis, K. W., Plattner, A., & Simons, F. J. (2015). A suite of software
506 analyzes data on the sphere. *Eos*, *96*. doi: 10.1029/2015EO025851
- 507 Harig, C., & Simons, F. J. (2012). Mapping Greenland’s mass loss in space and
508 time. *Proc. Natl. Acad. Sci. U. S. A.*, *109*(49), 19934–19937. doi: 10.1073/pnas
509 .1206785109
- 510 Harig, C., & Simons, F. J. (2015). Accelerated West Antarctic ice mass loss con-
511 tinues to outpace East Antarctic gains. *Earth and Planetary Science Letters*, *415*,
512 134–141. doi: 10.1016/j.epsl.2015.01.029
- 513 Harig, C., & Simons, F. J. (2016). Ice mass loss in Greenland, the Gulf of Alaska,
514 and the Canadian Archipelago: Seasonal cycles and decadal trends. *Geophysical*
515 *Research Letters*, *43*, 3150–3159. doi: 10.1002/2016GL067759
- 516 Harig, C., & Simons, F. J. (2022). csdms-contrib/slepian_delta: Release 1.2.1 [Com-
517 puter software]. Zenodo. Retrieved from [https://github.com/csdms-contrib/
518 slepian_delta](https://github.com/csdms-contrib/slepian_delta) doi: 10.5281/zenodo.6562354
- 519 Jiang, Z., Hsu, Y. J., Yuan, L., Yang, X., Ding, Y., Tang, M., & Chen, C. (2021).
520 Characterizing Spatiotemporal Patterns of Terrestrial Water Storage Variations
521 Using GNSS Vertical Data in Sichuan, China. *J. Geophys. Res. Solid Earth*,
522 *126*(12). doi: 10.1029/2021JB022398
- 523 Knappe, E., Bendick, R., Martens, H. R., Argus, D. F., & Gardner, W. P. (2019).
524 Downscaling Vertical GPS Observations to Derive Watershed-Scale Hydrologic
525 Loading in the Northern Rockies. *Water Resour. Res.*, *55*(1), 391–401. doi:
526 10.1029/2018WR023289
- 527 Knowles, L., Bennett, R. A., & Harig, C. (2020). Vertical displacements of the Ama-
528 zon basin from GRACE and GPS. *Journal of Geophysical Research: Solid Earth*,
529 *125*(2). doi: 10.1029/2019JB018105
- 530 Landerer, F. W., & Swenson, S. C. (2012). Accuracy of scaled GRACE terres-

- 531 trial water storage estimates. *Water Resour. Res.*, *48*(4), 1–11. doi: 10.1029/
532 2011WR011453
- 533 Loomis, B. D., Rachlin, K. E., Wiese, D. N., Landerer, F. W., & Luthcke, S. B.
534 (2020). Replacing GRACE/GRACE-FO With Satellite Laser Ranging: Im-
535 pacts on Antarctic Ice Sheet Mass Change. *Geophysical Research Letters*, *47*(3),
536 e2019GL085488. doi: <https://doi.org/10.1029/2019GL085488>
- 537 Love, A. E. H. (1909). The yielding of the Earth to disturbing forces. *Proc. R. Soc.*
538 *London Ser. A*, *82*(551), 73–88.
- 539 Martens, H. R., Rivera, L., & Simons, M. (2019). LoadDef: A Python-Based Toolkit
540 to Model Elastic Deformation Caused by Surface Mass Loading on Spherically
541 Symmetric Bodies. *Earth Sp. Sci.*, *6*(2), 311–323. doi: 10.1029/2018EA000462
- 542 Ouellette, K. J., De Linage, C., & Famiglietti, J. S. (2013). Estimating snow wa-
543 ter equivalent from GPS vertical site-position observations in the western United
544 States. *Water Resour. Res.*, *49*(5), 2508–2518. doi: 10.1002/wrcr.20173
- 545 Pedregosa, F., Varoquaux, G., Michel, V., Thirion, B., Grisel, O., Blondel, M., ...
546 Duchesnay, E. (2011). Scikit-learn: Machine Learning in Python. *J. Mach. Learn.*
547 *Res.*, *12*, 2825–2830. doi: 10.1289/EHP4713
- 548 Plattner, A., Kroeker, S., kyleejoford, hawerth6, & RamonRich. (2023).
549 Slepian/slepian: v1.2.0 [Computer software]. Zenodo. Retrieved from
550 <https://github.com/Slepian/Slepian> doi: 10.5281/zenodo.7838064
- 551 Ray, J., Altamimi, Z., Collilieux, X., & van Dam, T. (2007). Anomalous harmonics
552 in the spectra of GPS position estimates. *GPS Solutions*, *12*, 55–64. doi: 10.1007/
553 s10291-007-0067-7
- 554 Rebeschung, P., Altamimi, Z., Métivier, L., Gobron, K., & Chanard, K. (2024).
555 Analysis of the IGS contribution to ITRF2020. *Journal of Geodesy*, *98*(49). doi:
556 10.1007/s00190-024-01870-1
- 557 Rodell, M., Houser, P. R., Jambor, U., Gottschalck, J., Mitchell, K., Meng, C. J., ...
558 Toll, D. (2004). The Global Land Data Assimilation System. *Bull. Am. Meteorol.*
559 *Soc.*, *85*(3), 381–394. doi: 10.1175/BAMS-85-3-381
- 560 Simons, F. J., & Dahlen, F. A. (2006). Spherical slepian functions and the polar gap
561 in geodesy. *Geophys. J. Int.*, *166*(3), 1039–1061. doi: 10.1111/j.1365-246X.2006
562 .03065.x
- 563 Simons, F. J., & Harig, C. (2020). csdms-contrib/slepian_bravo: Release 1.0.4 [Com-
564 puter software]. Zenodo. Retrieved from [https://github.com/csdms-contrib/
565 slepian_bravo](https://github.com/csdms-contrib/slepian_bravo) doi: 10.5281/zenodo.4085221
- 566 Simons, F. J., Harig, C., & Plattner, A. (2020). csdms-contrib/slepian_alpha: Re-
567 lease 1.0.5 [Computer software]. Zenodo. Retrieved from [https://github.com/
568 csdms-contrib/slepian_alpha](https://github.com/csdms-contrib/slepian_alpha) doi: 10.5281/zenodo.4085210
- 569 Sun, Y., Riva, R., & Ditmar, P. (2016). Optimizing estimates of annual varia-
570 tions and trends in geocenter motion and j_2 from a combination of grace data
571 and geophysical models. *Journal of Geophysical Research: Solid Earth*, *121*(11),
572 8352–8370. doi: <https://doi.org/10.1002/2016JB013073>
- 573 Swenson, S. C., Chambers, D., & Wahr, J. (2008). Estimating geocenter variations
574 from a combination of grace and ocean model output. *Journal of Geophysical Re-
575 search: Solid Earth*, *113*(B8). doi: <https://doi.org/10.1029/2007JB005338>
- 576 Swenson, S. C., & Wahr, J. (2006). Post-processing removal of correlated errors in
577 GRACE data. *Geophys. Res. Lett.*, *33*(8), 1–4. doi: 10.1029/2005GL025285
- 578 Tapley, B. D., Bettadpur, S., Ries, J. C., Thompson, P. F., & Watkins, M. M.
579 (2004). GRACE measurements of mass variability in the Earth system. *Science*,
580 *305*(5683), 503–505. doi: 10.1126/science.1099192
- 581 Tregoning, P., & Watson, C. (2009). Atmospheric effects and spurious sig-
582 nals in GPS analyses. *J. Geophys. Res. Solid Earth*, *114*(9), 1–15. doi:
583 10.1029/2009JB006344
- 584 Tregoning, P., Watson, C., Ramillien, G., McQueen, H., & Zhang, J. (2009). Detect-

585 ing hydrologic deformation using GRACE and GPS. *Geophys. Res. Lett.*, *36*(15),
586 1–6. doi: 10.1029/2009GL038718

587 Tsai, V. C. (2011). A model for seasonal changes in GPS positions and seismic wave
588 speeds due to thermoelastic and hydrologic variations. *J. Geophys. Res. Solid*
589 *Earth*, *116*(4), 1–9. doi: 10.1029/2010JB008156

590 van Dam, T., Wahr, J., & Lavallée, D. (2007). A comparison of annual verti-
591 cal crustal displacements from GPS and Gravity Recovery and Climate Experi-
592 ment (GRACE) over Europe. *J. Geophys. Res. Solid Earth*, *112*(3), 1–11. doi:
593 10.1029/2006JB004335

594 von Hippel, M., & Harig, C. (2019). Long-term and inter-annual mass changes in
595 the Iceland ice cap determined from GRACE gravimetry using Slepian functions.
596 *Frontiers in Earth Science*, *7*(171), 1–10. doi: 10.3389/feart.2019.00171

597 Wahr, J., Molenaar, M., & Bryan, F. (1998). Time variability of the Earth’s gravity
598 field: Hydrological and oceanic effects and their possible detection using GRACE.
599 *J. Geophys. Res.*, *103*(B12), 30205–30229.

600 Wessel, P., Smith, W. H. F., Scharroo, R., Luis, J., & Wobbe, F. (2013). Generic
601 mapping tools: Improved version released. *Eos, Transactions American Geophys-
602 ical Union*, *94*(45), 409–410. doi: 10.1002/2013EO450001

603 White, A. M., Gardner, W. P., Borsa, A. A., Argus, D. F., & Martens, H. R. (2022).
604 A Review of GNSS/GPS in Hydrogeodesy: Hydrologic Loading Applications and
605 Their Implications for Water Resource Research. *Water Resources Research*,
606 *58*(7), e2022WR032078. doi: 10.1029/2022WR032078

607 Yan, H., Chen, W., Zhu, Y., Zhang, W., & Zhong, M. (2009). Contributions of
608 thermal expansion of monuments and nearby bedrock to observed GPS height
609 changes. *Geophys. Res. Lett.*, *36*(13), 1–5. doi: 10.1029/2009GL038152

610 Zeng, X., Broxton, P., & Dawson, N. (2018). Snowpack Change From 1982 to 2016
611 Over Conterminous United States. *Geophys. Res. Lett.*, *45*(23), 12,940–12,947.
612 doi: 10.1029/2018GL079621